

## THE CRATER WITH GRAVITY ANOMALY IN THE CENTER MAY BE THE ANCIENT VOLCANIC CRATER AND GEOTHERMAL UNDER IT

by

**Xiaoyi LI<sup>a</sup>, Wenliang DU<sup>a</sup>, Hanwen CUI<sup>b</sup>, and Xiaolin TIAN<sup>a\*</sup>**

<sup>a</sup> Macau University of Science and Technology, Avenida Wai Long, Taipa, Macau

<sup>b</sup> Zhuhai College of Jilin University, Jinwan, Zhuhai, Guangdong, China

Original scientific paper

<https://doi.org/10.2298/TSCI181210190L>

*Lunar volcanism play an important role on studying the thermal and compositional evolution of the Moon. However, the studies on the relationships among composition, location and age of Lunar volcanos are still limit. The high-quality and multi-source remote sensing data offer the opportunity to obtain significant features of the Lunar volcanism and the evolution of the Moon. Specifically, the high-quality gravitational features of volcanic landforms of the Moon are observed by the Gravity Recovery and Interior Laboratory. Besides, the lunar reconnaissance orbiter camera provides detail morphologic features of Lunar volcanos based on high-resolution optical images. This paper aims to find the characteristic of lunar volcanos by observing the gravitational and morphologic features in the center of craters. The final results show that most of the craters with central peaks have gravity anomalies except the Mendeleev crater (5.7 °N and 140.9 °E) whose central area contains significant gravity anomalies but no central peaks. The area of gravity anomaly may indicate heat source under the ground.*

Key words: ancient volcanic crater, fast detection, gravity anomaly

### Introduction

The material composition and structure of the deep moon shell and the moon mantle are one of the key issues in today's lunar science [1]. It is important for us to understand the early lunar formation and to explore the cause of the dichotomy of the moon (the obvious differences in the topography, structure, material composition, and thickness of the moon shell on the front and back of the moon). However, it cannot directly obtain accurate components of the deep moon shell and the moon mantle through remote sensing. Rock samples from the deep moon have not been collected either. Data such as moon-shock, lunar gravity and topography are used for deep structures research.

The US Gravity Recovery and Interior Laboratory (GRAIL) launched at the end of 2011. High precision lunar gravity data obtained by the detector [2]. Gravity data uses the latest published 1500 order spherical harmonic model. The effective gravity is 900 orders [3, 4]. The thickness of the moon shell is an important parameter for studying the formation and evolution of the moon. Use the GRAIL and LRO terrain data, Wieczorek *et al.* [5] calculated the shell thickness model. This model comprehensively analyzes the thickness and distribution of the moon shell. This model analyzes the thickness and distribution of the moon shell, based on the

\* Corresponding author, e-mail: xltian@must.edu.mo

average monthly shell thickness obtained from Apollo 12 and 14 month seismic observation data. Qian and Wieczorek [6] calculated the average density of the moon shell as 2550 and gave four different calculation model results.

The moon crater is formed by the small planet hitting the Moon. The spatial distribution characteristics of the crater provide useful reference for understanding the impact different periods of lunar evolution [7], the asteroid impact process, and the determination of lunar soil thickness [8]. At present, based on the basic idea of the crater extraction algorithm, the identification method can be divided into the following three: the identification method of lunar crater based on the lunar surface terrain, the identification method of compared gray difference pixels' value based on impact crater on remote sensing image, and the identification method is to integrate remote sensing image and terrain information. Among them, the first method is mainly based on the DEM data, using the terrain comprehensive analysis [9], simulated lava flow characteristics [10] and other methods to extract the impact crater. The advantage is that it can effectively identify the morphological features of the crater. However, due to the low resolution of early DEM data, the small crater recognition was very bad. For the remote sensing image, many scholars use edge detection [11], genetic search algorithms [12] to extract crater images. Then using hough transform or least squares to fit and match the crater. However, due to the influence of the angle and height of the light and the complex terrain of the crater, the extracted crater edge does not completely match the actual undulation position. The recognition accuracy is not high. As the resolution of DEM data increased, some scholars began to explore the detection algorithms using the remote sensing image and DEM data [13].

This paper first quotes gravity anomaly analysis in the Von Kaarman crater. The *Chang'e-4* spacecraft is about to land this crater. This paper found an algorithm for quickly identifying craters. Analysis result, there is a crater without central peak, but it with the gravity anomaly like the Von Karman crater. This crater is Mendeleev crater on the back of the moon. This area may be have some mantle material like Von Karman crater.

## Gravity and terrain

### *Gravity and terrain related functions*

The gravity and terrain of the planet are usually expressed in the form of spherical harmonics function.

$$g(\theta, \phi) = \sum_{l=0}^{\infty} \sum_{m=-l}^l g_{lm} Y_{lm}(\theta, \phi) \quad (1)$$

$$h(\theta, \phi) = \sum_{l=0}^{\infty} \sum_{m=-l}^l h_{lm} Y_{lm}(\theta, \phi) \quad (2)$$

where  $l$  is the order of the spherical harmonic function,  $m$  – the harmonic of the spherical harmonic function,  $g$  – the gravity spherical harmonic parameter,  $h_{lm}$  – the terrain spherical harmonic parameter. The admittance  $Z(l)$  (admittance) and related  $\gamma(l)$  (correlation) of the frequency domain gravity and terrain can be expressed:

$$Z(l) = \frac{S_{hg}(l)}{S_{hh}(l)} \quad (3)$$

$$\gamma(l) = \frac{S_{hg}(l)}{\sqrt{S_{hh}(l)S_{gg}(l)}} \quad (4)$$

where  $S_{hg}(l)$  is cross power spectrum for gravity and terrain,  $S_{hh}(l)$  – gravity autocorrelation spectrum, and  $S_{gg}(l)$  – terrain autocorrelation spectrum.

In the frequency domain, the relationship between gravity and terrain can usually be expressed:

$$g_{lm} = Q_{lm} h_{lm} + I_{lm} \quad (5)$$

where  $Q_{lm}$  is a linear conversion equation and  $I_{lm}$  – part of the gravity field information that is not represented by the model. The main data is the noise in the gravitational field. Assume that  $I_{lm}$  is not related to terrain. Calculate the spectral information of gravity and terrain  $S_{hg}(l)$ ,  $S_{gg}(l)$ ,  $S_{hh}(l)$ , and the ratio relationship admittance  $Z(l)$  and related  $\gamma(l)$  using eqs. (3) and (4). Create a gravity and topographic relationship model  $Q_{lm}$ . Use this relational model to get the simulated spectral information fit the actual spectral data. So it can obtain the geophysical parameters. Assume that the lithosphere of the planet is a thin elastic spherical shell. If the terrain surface is a carrier, it can obtain the linear transformation model  $Q_{lm}$  for gravity and terrain:

$$Z(l) = f(\rho_c, \rho_m, \nu, E, T_e, T_c, z, g, R) \quad (6)$$

$$\gamma(l) = 1 \text{ or } -1 \quad (7)$$

Obviously, the admittance is shell density,  $\rho_c$ , mantle density,  $\rho_m$ ,  $\nu$  is the poisson's ratio,  $E$  – the young's modulus,  $T_e$  – the elastic thickness,  $T_c$  – the moon shell thickness,  $z$  – the burial depth,  $g$  – the planetary gravity, and  $R$  – planet radius. These parameters can be solved by comparing the measured and the model admittance values.

#### Von Karman crater

China will launch the *Chang'E 4* lunar exploration satellite at the end of 2018. A large amount of magma invaded after the formation of the crater. Snape *et al.* [14] think that the western region of Von Karman crater is a volcano, fig. 1. Snape *et al.* [14] uses the terrain and gravity data acquired by the early Japanese *Moon Goddess*. This area may be as the first landing area for the von Karman crater. Analysis shows that the thickness of the moon shell in the SPA area is thin. This area may collect basalt samples from the moon cellar.

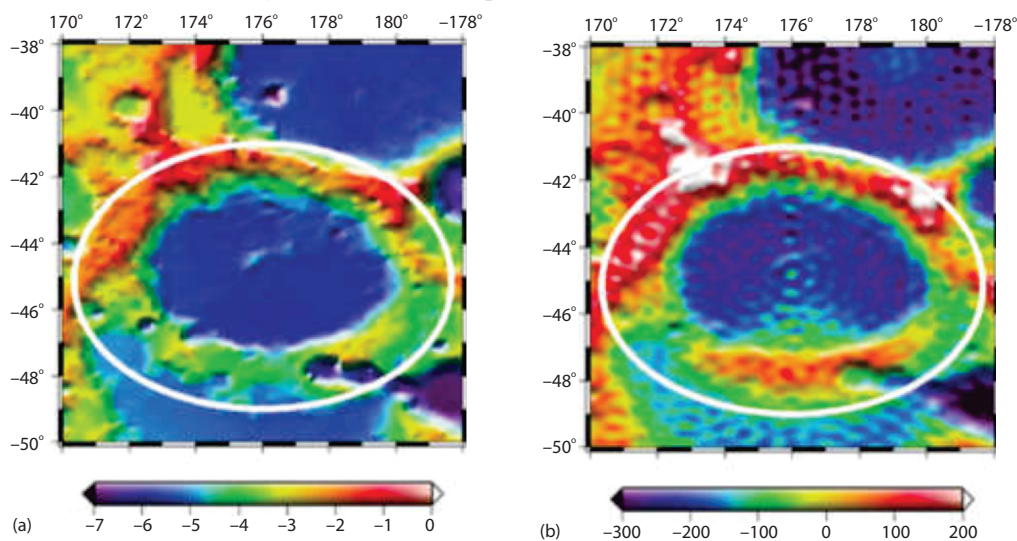


Figure 1. Von Karman crater DEM data and gravity anomaly

### Gravity and terrain data

The terrain and gravity data used in this study are all from the planetary data system. (Planetary Data System, <http://pds-geosciences.wustl.edu/>). The terrain data comes from the laser altimeter LOLA mounted on the LRO. The 2050 order spherical harmonic model is used. ([http://pds-geosciences.wustl.edu/lro/lro-1-lola-3-rdr-v1/lrolol\\_1xxx/data/lola\\_shadr/](http://pds-geosciences.wustl.edu/lro/lro-1-lola-3-rdr-v1/lrolol_1xxx/data/lola_shadr/)). The US Gravity Recovery and Interior Laboratory launch-ed at the end of 2011. Unprecedented high precision lunar gravity field detection data obtained by the detector. Therefore, the gravity field data uses the newly published 1500 order spherical harmonic model ([http://pds-geosciences.wustl.edu/grail/grail-1-lgrs-5-rdr-v1/grail\\_1001/shadr/](http://pds-geosciences.wustl.edu/grail/grail-1-lgrs-5-rdr-v1/grail_1001/shadr/)). The model uses data from all GRAIL observation arcs. Bouguer gravity and gravity gradient.

In the space domain Cartesian co-ordinate system, the second-order horizontal gradient component of the Bouguer gravity bit can be represented by  $\Gamma_{yy}$ ,  $\Gamma_{xx}$ ,  $\Gamma_{xy}$ . Two eigenvalues  $\Gamma_{11}$  and  $\Gamma_{22}$  of the Bouguer gravity horizontal gradient tensor can be calculated. Representing the maximum and minimum curvature of the Bouguer gravity position. Normalize the two eigenvalues to obtain the maximum horizontal gradient value:

$$\Gamma_{hh} = \begin{cases} \Gamma_{11} & \text{if } \Gamma_{11} > \text{abs}(\Gamma_{22}) \\ \Gamma_{22} & \text{if } \Gamma_{11} < \text{abs}(\Gamma_{22}) \end{cases} \quad (8)$$

The Bouguer gravity gradient is the second derivative of gravity anomaly and can be used to extract some linear features and correspond to the subsurface fault structure, the boundary zones of different lithologic geologic, and other structures with density differences, fig. 2.

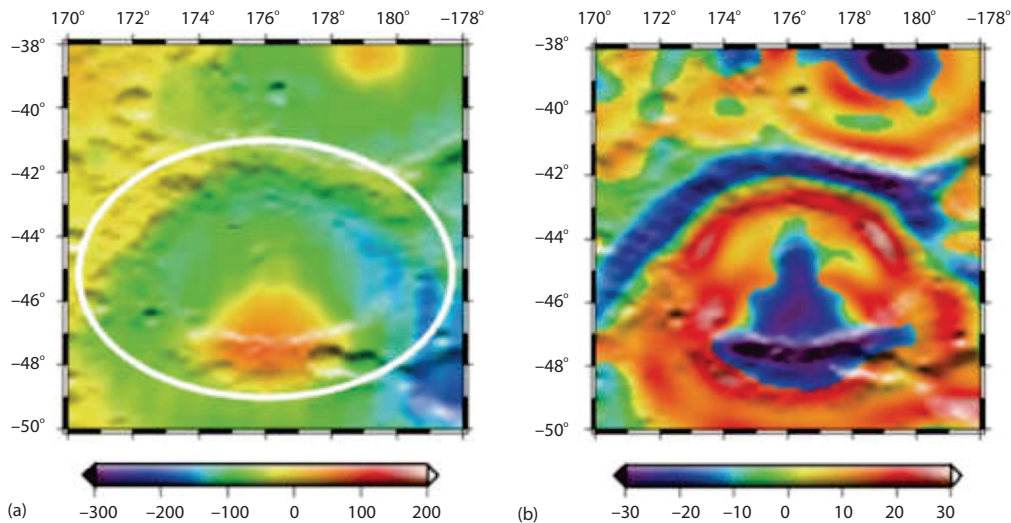


**Figure 2.** Bouguer gravity anomaly and Bouguer gravity gradient anomaly map of Von Karman crater [15]; Bouguer gravity anomaly (b) Bouguer gravity gradient anomaly

### Lunar crater

On the Moon, the crater is a major common annular structure. The number of small celestial craters that can be confirmed at present is about 170. These craters range in diameter from 100 m to 300 km. There are two typical impact craters on remote sensing images. The Bowl-shaped impact crater is a young crater. It is the common crater and the number is the most. The central-peak impact crater caused by geological reasons.

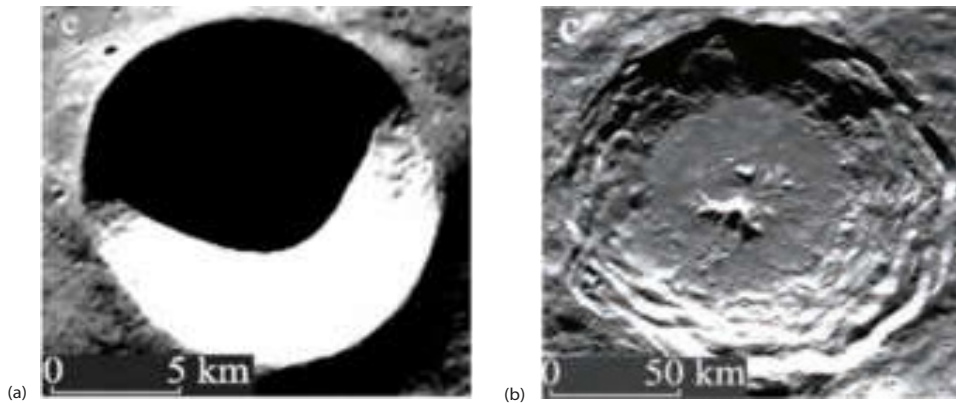


Figure 3. (a) Bowl-shaped impact crater, (b) central-peak impact crater

From the fig. 3 we can see that the impact crater is greatly affected by the illumination. During the photographing of the CCD camera, the illumination cannot be directed to the crater vertically. So there is a light shadow in the crater image. Due to the angle of incident light, the area of the shadow is different. Some scholars believe that the angle of incidence of sunlight can be derived from the size of the shadow area and the DEM data. The shadows can reflect some of the information at the bottom of the crater.

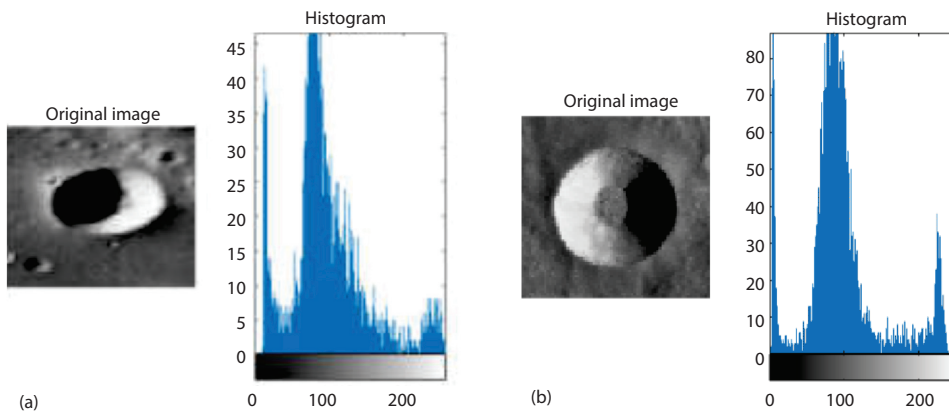


Figure 4. The histogram of the lunar impact affected by light

There are two crater image found on the surface of the Moon, and two histogram statistics for these two images, fig. 4. One incident light angle of the image is bigger than another. Histogram statistics for these two images. The result shows that most of the pixel values are around 100. This is because the normal pixels expressed by most of the rocks on the surface of the Moon. These pixels are the most common gray values in lunar soil. But there are also many pixel values near the minimum and maximum values of the pixel values. This is due to the influence of light. In these areas, pixels are minimally affected by terrain. These minimum and maximum value pixels appear at the edge of the crater. Positioning the crater by locating the pixel area of the maximum and minimum values.

But for some very small impact craters, the number of pixels is small. They will not show the same statistical results as previous. They reflect the geological information is very little. Therefore, those smaller impact craters will not be considered. In addition the crater, images of other topo-

graphical features also have this phenomenon, such as moon hills, moon streams, moon ridges. This phenomenon is mainly caused by the difference in the topography of the moon's surface.

### Convolutional neural network

A convolutional neural network is a type of multi-layer supervision learning network, which includes the input layer, hidden layer and output layer, where the hidden layer (comprising the convolution layer and down-sampling layer) is the important link of the deep extraction feature by the convolutional neural network:

$$x_j^l = f \left( \sum_{i \in M_j} x_i^{l-1} k_{ij}^l + b_j^l \right) \quad (9)$$

where  $l$  is the number of layers,  $k$  – the convolution kernel,  $M_j$  – the range of the input layer, and  $b$  – the bias value.

The form of the lower sampling layer:

$$x_j^l = f \left[ \beta_j^l p(x_i^{l-1}) + b_j^l \right] \quad (10)$$

where  $p$  is the pooling function and  $\beta$  – the weight.

The weight-sharing structure of the convolutional neural network makes it more similar to the biological neural network to decrease the complexity of the network model, reduce the weight quantity and be consistent with the topological structure of input images and networks in image processing for feature extraction and pattern classification.

### Central peak determination

An impact crater with a central peak is a special terrain for an ordinary crater. The difference is that the bottom of the crater has a central peak. We can distinguish the central peak impact crater by calculating the center roughness of the bottom of the crater. Roughness is a simple parameter for determining terrain. The higher of the center roughness, the less smooth of the crater.

$$R_{mn} = \sum_{i=m}^{m+2n+2} \sum_{j=n} |X_{m+1,n+1} - X_{ij}| \quad (11)$$

where  $R$  is the roughness and  $X_{ij}$  – the center pixel value.

There is a simple definition of the degree of roughness. The roughness calculate the sum of the difference between the center point and his neighbor. The larger the value, the greater difference between this pixel and his neighbor.

### Lunar impact crater detection

Next, we will introduce the framework design of the convolutional god network (such as the every layer type, the training parameters of dimension and regularization). First, there are 60 crater images. They are the training samples. But the samples is less than ordinary experiment. The samples used be change to add the samples. The samples have be reversed and partial interception, fig. 5.

We design the following network structure in order to ensure the full link of the convolutional neural network. The first layer convolution kernels is  $5 \times 5 \times 1 \times 20$ . There are 20 maps in the first layer. So the second layer convolution kernels is  $5 \times 5 \times 20 \times 50$ . After the training, we only identified the crater. Then using the roughness parameter to distinguish the central peak impact craters, fig. 6.

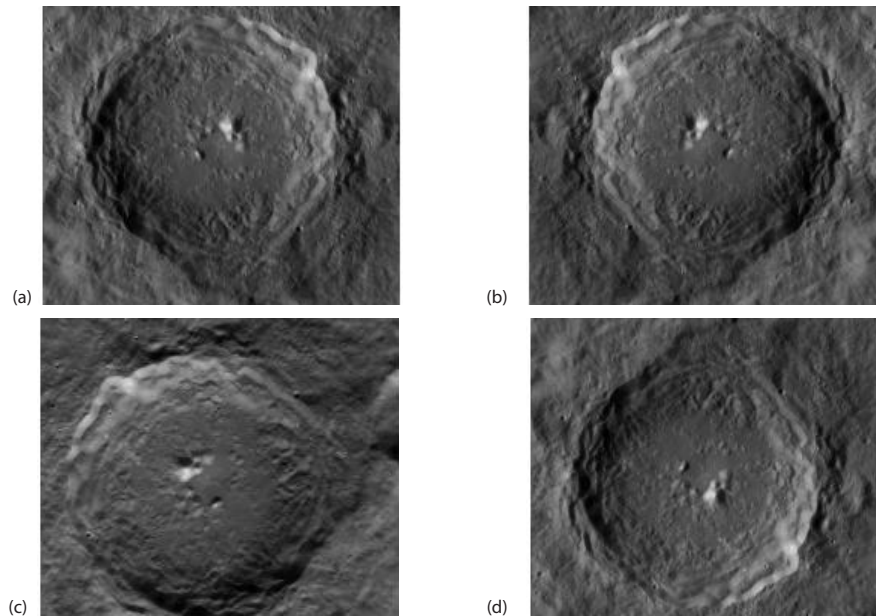


Figure 5. Extended sample; (a) original image, (b) vertical reversal, (c) 90° reversal, and (d) horizontal reversal

#### Gravity anomaly area

Through the previous algorithm we can quickly get the location of the crater. But some of the crater without the central peak. These craters also have the high roughness. As shown fig 7.

Although these images are wrong craters, they are may also be a suspected crater. When the Moon is hit by a foreign planet, at the bottom of the crater may form cracks, as fig. 7(c). First, for the central peak crater, there are gravity anomaly at the central re-

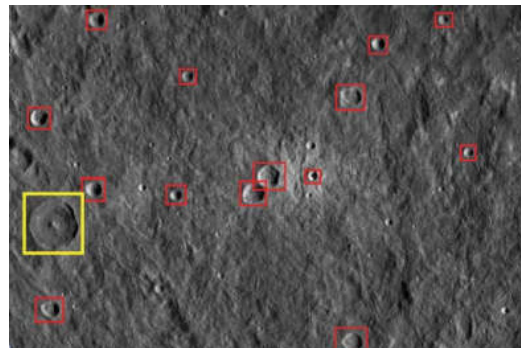


Figure 6. The result of the identification of the crater

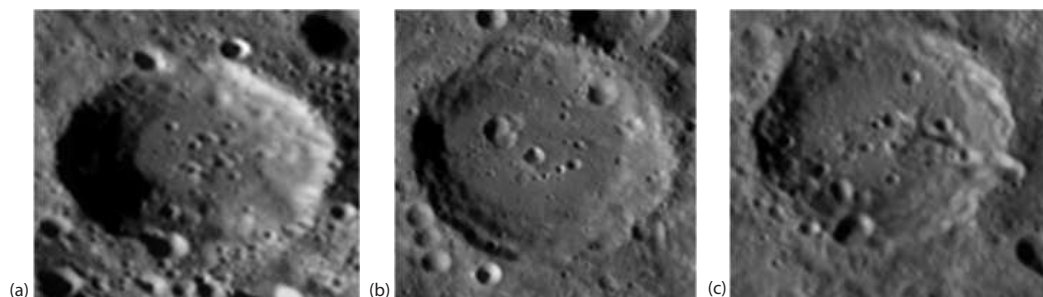
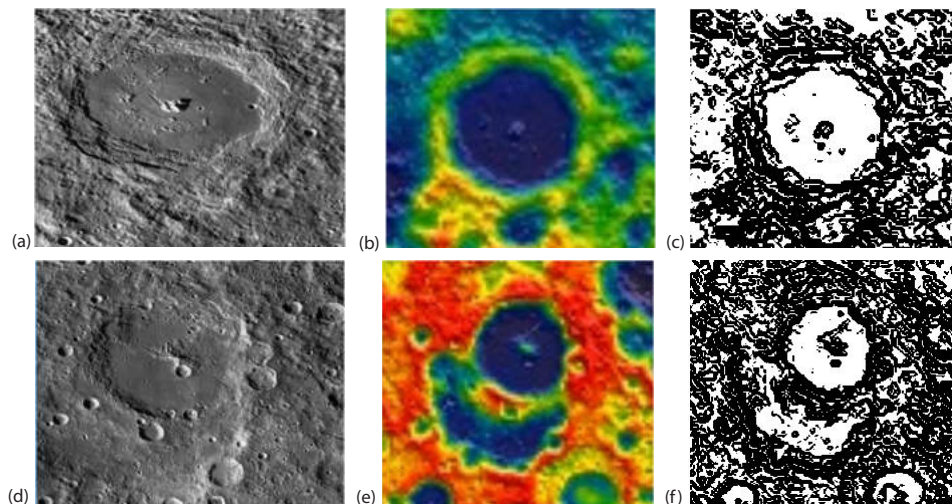


Figure 7. Considered to be a crater with a central peak; (a) misidentified crater 1 (b) misidentified crater 2 (c) misidentified crater 3

gion. Gravity anomalies can reflect the superficial matter of the Moon. Gravity anomalies may be caused by magma overflow of the mantle.

Although these images are wrong craters, they are may also be a suspected crater. When the Moon is hit by a foreign planet, at the bottom of the crater may form cracks, as figs. 8(c) and 8(f). First, for the central peak crater, there are gravity anomaly at the central region. Gravity anomalies can reflect the superficial matter of the Moon. Gravity anomalies may be caused by magma overflow of the mantle.



**Figure 8. Two craters with a central peak; (a) CCD image, (b) gravity anomaly, (c) gravity anomaly gradient, (d) CCD image, (e) gravity anomaly, and (f) gravity anomaly gradient**

As fig. 9(c) shown that there are the gravity anomaly at the center. This situation like the Von Karman crater. But in the wrong identification crater there are also the gravity anomaly. Although there are some tiny craters here at the bottom of the crater. The gravity anomaly is not cause by the terrain. The edge of the crater is blurred, so it is a ancient crater. In its southeast direction, there is a crater with central peak.

### **Discuss and conclusion**

The *Chang'e-4* satellite will land in the Von Karman crater in the SPA basin on the back of the Moon at end of the 2018, and it is expected to achieve the mantle material. Comprehensive research on the Von Karman crater, the central peak. The formation of the central peak is due to the overflow of the lunar material. In our identification of the impact crater, many craters with complex terrain at the crater bottom are found. Many of them may be suspect volcanic crater on the image. The distribution of moon mantle may reflect moon internal structure. It is good for us study the evolution of the Moon.

In this paper, there is a crater region that it without the central peak, but it with the gravity anomaly. This crater is Mendeleev crater. The edge of the crater is blurred, so it is an ancient crater. At the botton of the crater, there are soma youth small crater, too. The gravity anomaly reflected the different substances in the near surface. There are some carters with central peak near it. There is not much research on the back of the moon. Perhaps this crater may be a breakthrough for humans study.

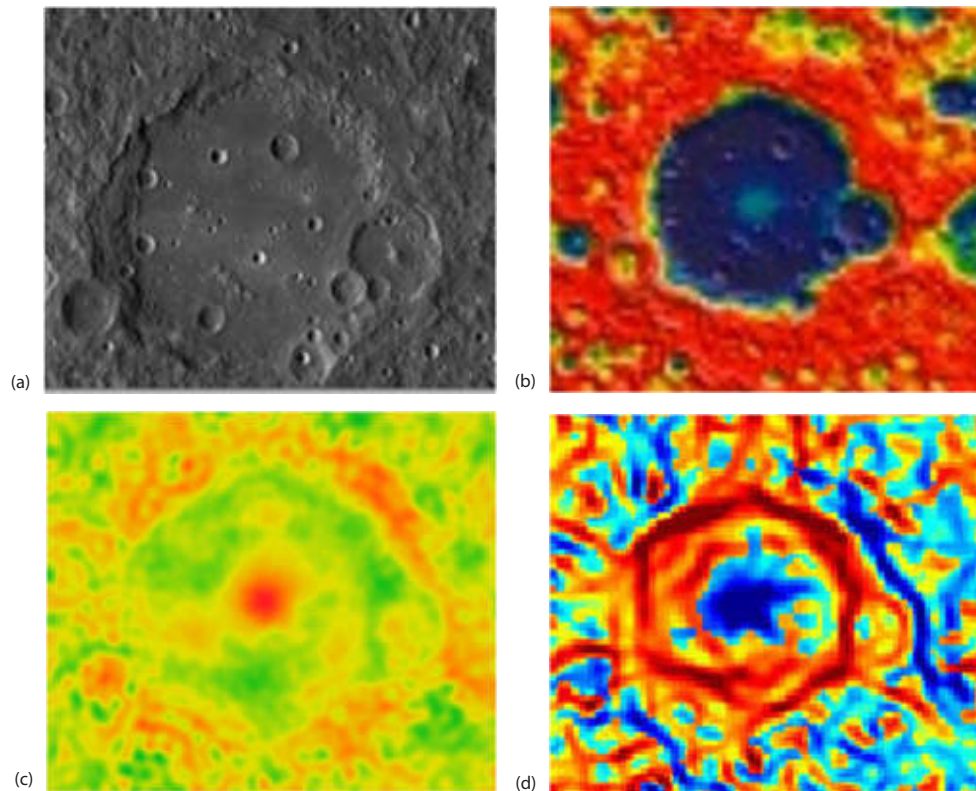


**Figure 9.** The Mendeleev crater; (a) CCD image, (b) gravity anomaly image, (c) Bouguer gravity image, and (d) Bouguer gravity anomal

The internal temperature distribution of the moon is an important parameter for determining the physical state and chemical composition of the Moon. It is not possible to directly measure the internal temperature of the Moon. But the gravity data can reflect the Rock distribution of the lunar surface. There may be an overflow of magma flow in areas of greater gravity anomalies. The rock properties of these areas may reflect the evolution of moon mantle and moon core.

### Acknowledgment

We would like to show our deepest gratitude to the Science and Technology Development Fund of Macao (No. 99/2016/A3) for their strong financial support.

### References

- [1] \*\*\*, Board, Space Studies, and National Research Council, The Scientific Context for Exploration of the Moon, National Academies Press, Washington DC, 2007
- [2] Zuber, M. T., *et al.*, Gravity Field of the Moon from the Gravity Recovery and Interior Laboratory (GRAIL) Mission, *Science*, 339 (2013), 6120, pp. 668-671
- [3] Konopliv, A. S., *et al.*, High-Resolution Lunar Gravity Fields from the GRAIL Primary and Extended Missions, *Geophysical Research Letters*, 41 (2014), 5, pp. 1452-1458
- [4] Lemoine, F. G., *et al.*, The GRGM900C: A Degree 900 Lunar Gravity Model from GRAIL Primary and Extended Mission Data, *Geophysical Research Letters*, 41 (2014), 10, pp. 3382-3389

- [5] Wieczorek, M. A., *et al.*, The Crust of the Moon as Seen by GRAIL, *Science*, 339 (2013), 6120, pp. 671-675
- [6] Qian, Q., Wieczorek, M. A., Density and Porosity of the Lunar Crust from Gravity and Topography, *Journal of Geophysical Research: Planets*, 117 (2012), E05003
- [7] Michael, G. G., Gerhard, N., Planetary Surface Dating from Crater Size-Frequency Distribution Measurements, Partial Resurfacing Events and Statistical Age Uncertainty, *Earth and Planetary Science Letters*, 294 (2010), 3-4, pp. 223-229
- [8] Di, K., *et al.*, Lunar Regolith Thickness Determination from 3-D Morphology of Small Fresh Craters, *Icarus*, 267 (2016), Mar., pp. 12-23
- [9] Bue, B. D., Tomasz, F., Stepinski. Machine detection of Martian Impact Craters from Digital Topography Data, *IEEE Transactions on Geoscience and Remote Sensing*, 45 (2007), 1, pp. 265-274
- [10] Degirmenci, M., Shatlyk, A., *Impact Crater Detection on Mars Digital Elevation and Image Model*, Middle East Technical University, Ankara, Turkey, 2010
- [11] Vijayan, S., K. *et al.*, Crater Detection, Classification and Contextual Information Extraction in Lunar Images Using a Novel Algorithm, *Icarus*, 226 (2013), 1, pp. 798-815
- [12] Cohen, J. P., Wei, D., Crater Detection Via Genetic Search Methods to Reduce Image Features, *Advances in Space Research*, 53 (2014), 12, pp. 1768-1782
- [13] Salamunićar, G., *et al.*, Hybrid Method for Crater Detection Based Onpography Reconstruction from Optical Images and the New LU78287GT Catalogue of Lunar Impact Craters, *Advances in Space Research*, 53 (2014), 12, pp. 1783-1797
- [14] Snape, J. F., *et al.*, Science-Rich Mission Sites within South Pole-Aitken Basin – Part 2: Von Karaman Crater, *Proceedings, 41<sup>st</sup> Lunar and Planetary Science*, Woodlands, Tex., USA, 2010
- [15] Huang, Q., *et al.*, Crustal and Subsurface Structures of Chang'e-4 Lunar Farside Landingsite, *Journal of Deep Space Exploration*, 5 (2018), 1, pp. 41-49